Formation Mechanisms of Covalent Nanostructures from Density Functional Theory

Jonas Björk

Abstract In this chapter, it is demonstrated how electronic structure calculations, with focus on density functional theory, can be used to gain insight about on-surface reactions. I first give a brief introduction to how density functional theory can be used to study reactions. The focus is then shifted to two different types of on-surface reactions, highlighting the theoretical work that has been performed to gain detailed atomistic insight into them. First, the state of the art of the theory behind on-surface Ullmann coupling is described. In this reaction, molecular building blocks dehalogenate, which enables them to covalently couple. The most crucial reaction parameters are identified—the diffusion and coupling barriers of surface-supported radicals—and the potential for theory to optimize these is discussed. We then concentrate on the homo-coupling between terminal alkynes, a rudimentarily different process where molecules initially couple before undergoing a dehydrogenation step. The theory of the mechanism behind this coupling strategy is less developed than that of the on-surface Ullmann coupling, where fundamental questions remain to be unraveled. For example, by the subtle change of substrate from Ag to Au, the on-surface alkyne chemistry is completely altered from the homo-coupling to a cyclodehydrogenation reaction for the same molecular building block, of which origin remains unknown. The main objective of the chapter is to give an impression of what kind of information theory can obtain about reaction on surface, as well as to motivate and inspire for future theoretical studies, which will be needed to turn on-surface synthesis into a more predictive discipline.

J. Björk (✉)
Department of Physics, Chemistry and Biology, IFM, Linköping University, Linköping, Sweden
e-mail: jonas.bjork@liu.se; jonbj@ifm.liu.se

A. Gourdon (ed.), *On-Surface Synthesis*, Advances in Atom and Single Molecule Machines, DOI 10.1007/978-3-319-26600-8_13

1 Introduction

As demonstrated throughout this book, on-surface synthesis is a versatile tool for tailoring novel covalent nanostructures. At the moment, though, it is difficult to predict how a molecule will react on a surface, mainly due to that the on-surface reactions in many cases behave rudimentarily different from their wet chemistry counterparts. In order to make use of the true potential of the on-surface synthesis approach toward covalent nanostructures, we need to gain full control over each step of the relevant on-surface reaction protocols. An important course of action toward such a control is the detailed understanding of the reaction mechanisms governing the various on-surface synthesis strategies. Such information is in most often not accessible from experiments, due to short-lived transition and intermediate states of the reactions. Instead, atomic-level theoretical modeling is employed to study reaction mechanisms of on-surface synthesis. The immediate impact of such theoretical modeling is to establish a chemical intuition of on-surface reaction that is currently missing, aiding surface scientists in making more qualified choices when designing their experiments.

This chapter aims to highlight some of the work that has been performed from theory to obtain an understanding of the fundamental mechanisms underlying on-surface reactions. We will further identify questions of particular importance about on-surface synthesis, which theory will have to encounter during the forthcoming years. The chapter is divided into three main parts: First, it will be briefly discussed how density functional theory can be used to study reaction mechanisms. Secondly, the current state of the art of the theory behind on-surface Ullmann coupling will be discussed. Finally, the complexity of on-surface synthesis will be demonstrated, showing a completely different type of coupling scheme recently introduced [33], namely the homo-coupling of terminal alkynes. The chapter is concluded by a brief outlook.

2 Studying Reaction Mechanisms with Density Functional Theory

The method of choice for studying on-surface reactions is density functional theory (DFT), which is basically the highest level of theory that is numerically affordable for treating the adsorption of relatively large organic molecules on surfaces. Furthermore, it has been successful in studying reactions relevant to heterogenous catalysis, such as ammonia synthesis [27]. In DFT, the total energy of a system is calculated as a functional of the electron density $n(\mathbf{r})$ [24]

$$E[n(\mathbf{r})] = T_s[n(\mathbf{r})] + \int \mathrm{d}\mathbf{r}\, v(\mathbf{r}) n(\mathbf{r}) + \frac{1}{2}\int \mathrm{d}\mathbf{r}\mathrm{d}\mathbf{r}' \frac{n(\mathbf{r})n(\mathbf{r}')}{|\mathbf{r}-\mathbf{r}'|} + E_{xc}[n(\mathbf{r})], \qquad (1)$$

where the first term is the kinetic energy of non-interacting electrons, the second and third terms give the electron-nuclei and electron-electron Coloumb energy, respectively, and the final term is the so-called exchange-correlation (XC) energy. All these terms can be determined exactly, except for the XC energy, which has to be approximated. Popular approximations include for example the local density approximation and the generalized gradient approximation.

An important point when computing molecules on surfaces with DFT is how to treat the so-called van der Waals (vdWDF) interactions, or London dispersion forces. By construction, the conventionally used generalized gradient approximation and local density approximation fail to describe these interactions, with the result that adsorption heights are generally overestimated for weakly adsorbed systems, which may result in that the computed reactivity between a molecule and a surface is not described correctly. Two main schools of thought for treating vdW interactions have emerged: dispersion-corrected DFT [18, 31] and the van der Waals density functional [12, 32]. Without going into any details about either of the methods, considering their most recent advances, both approaches have demonstrated the ability of describing adsorption heights with an accuracy of about 0.1 Å [4, 7, 28, 31].

The relevant reactions for on-surface synthesis are often rare-event processes, occurring at rates order of magnitudes smaller than typical vibrational frequencies of molecules. Simulating the complete atomistic dynamics of these reactions at the DFT level of theory is therefore not computationally feasible, nor even possible with state-of-the-art computational resources in most cases, and we have to relate on alternative methods. The work presented in this chapter has all been performed with transition state theory, where we describe a reaction by the energy at the initial state, the final state, and the transition state, which is the lowest-energy saddle point separating the final from the initial state.

2.1 Methods for Finding Transition States

The initial and final states of a reaction are local minima at the potential energy surface, which can be found by means of standard minimization algorithms. Finding a transition state, which is a saddle point at the potential energy surface, is less straightforward and requires minimization algorithms with special constraints ensuring that a saddle point, rather than a local minimum, is found. There are several methods for finding transition states using electronic structure theory, which can be divided into two groups: chain of state methods and minimum mode following methods.

The most popular chain-of-state method is probably the nudged elastic band (NEB) method [21], including the climbing image NEB (CI-NEB) [22], which is a slightly tweaked version of NEB for more efficient convergence of transitions states. In the NEB method, one starts from an initial guess of the reaction path, leading from the initial to the final state. The path is represented by a number of

images (atomic configurations). The reaction path is optimized by minimizing the forces on the atoms of each image perpendicular to the tangent of the path (nudging). Furthermore, images are kept separate from one another by springs (elastic bands). In the CI-NEB method, the spring force is removed for the image with highest energy and is replaced with the negative of the force parallel to the tangent of the path [22]. This way, the highest energy image is forced to move up-hill along the path toward the saddle point. In other words, the highest energy image converges toward the transition state of the reaction pathway. It should be noted that a reaction path determined by the NEB methods depends on the initial guess of the path (how we interpolate between initial and final states). Depending on the type of reaction, we may need to consider several initial guesses when calculating reaction paths with NEB and CI-NEB.

With some caution, the NEB and CI-NEB methods present reliable ways of optimizing reaction paths, and in particular they provide information of how many barriers separate the initial and final states. However, they rely on an accurate tangent of the reaction path (determined by finite differences between images) and thus require a sufficient number of images to converge the reaction path. Therefore, the method becomes numerically expensive since an individual DFT calculation is needed for each image. Minimum mode following methods, which we exemplify by the Dimer method [20, 23], provide a numerically cheaper approach since we focus on the optimization toward a transition state without having the information about the complete reaction path. Using the Dimer method, there are different ways to make an initial guess for the calculation. We can either move the dimer in different directions from the initial state (even without knowledge of the final state), interpolate between initial and final states, or use the results from a NEB calculation to initialize the calculation. For complex multidimensional reactions, often encountered in on-surface synthesis, the last alternative is most appealing, since we have the full trajectory between initial and final states from NEB and thus know how many barriers separate the final from the initial state, and we use for example the Dimer method to refine the transition state(s) found from NEB.

2.2 *A Recipe for Efficient Reaction Path Determination Using the Nudged Elastic Band and Dimer Methods*

In the previous section, we deduced that the NEB and Dimer methods in combination give a reliable method for finding the transition states separating an initial and a final state of a reaction. It should nevertheless be noticed that all barriers found with DFT should be taken with caution since they to some extent will depend on the employed exchange-correlation functional. If we play with the idea that our density functionals can be trusted, which is certainly not always the case, the *recipe* for finding transition states along for a reaction goes as follows:

1. Determine initial and final states of the reaction (high numerical accuracy).
2. Interpolate between initial and final states to obtain an initial guess for the reaction path.
3. Use the NEB method to preoptimize the reaction path (low numerical accuracy). If a multibarrier reaction is found, divide the overall reaction into several sub-paths and return to point 1 for each of these paths.
4. Use the CI-NEB method [21] to further optimize the reaction path and find an initial guess of the transition state (low numerical accuracy).
5. Use the Dimer method to optimize the initial guess of the transition state obtained in Step 4 (high numerical accuracy).

The numerical accuracy for each step refers to for example the size of basis set and the *k*-point sampling used in the calculations. A relatively low numerical accuracy may be used for the NEB and CI-NEB calculations, since we are mainly interested in determining the number of barriers of the reaction, and obtaining initial guesses for transition states to be used as input in the Dimer method. Thus, we only need to describe the pathway with NEB and CI-NEB at a qualitative level. Numerically converged reaction energies and energy barriers are ensured by the high numerical accuracy in the calculations of initial and final states, as well as of the transition state using the Dimer method.

Already at point 1 in the above *recipe*, we can calculate the overall reaction energy according to

$$E_{\text{react}} = E_{\mathbf{FS}} - E_{\mathbf{IS}}, \tag{2}$$

where $E_{\mathbf{IS}}$ and $E_{\mathbf{FS}}$ are the energies of the initial and final states, respectively. Finally, after optimizing the transition state in Step 5, we can calculate the energy barrier of the reaction

$$E_{\text{barrier}} = E_{\mathbf{TS}} - E_{\mathbf{IS}}, \tag{3}$$

where $E_{\mathbf{TS}}$ is the energy of the transition state.

3 Theory of On-Surface Ullmann Coupling

The Ullmann-type coupling is probably the most frequently used reaction scheme in on-surface synthesis. Within the concept of covalent organic nanostructures, it was introduced by Grill et al. in 2007 [17], who shown that porphyrins can be coupled into 0D, 1D, and small 2D structures, depending on the number of halogens attached to each molecular precursor. Since then, it has been used numerous of times to form different types of structures [11, 14, 25], such as porous graphene [1], and atomically precise graphene nanoribbons [8]. It should, however, be noted that the principle of on-surface Ullmann coupling was proven earlier for the formation of biphenyl from iodobenzene on Cu(111) [34].

The on-surface Ullmann coupling is conceptually easy to grasp. Firstly, halogen-substituted molecules are deposited on a surface. Since the halogen–carbon bonds are more easily dissociated than other intramolecular bonds, for example carbon–hydrogen bonds, it is possible to tune the temperature such that only the halogens are abstracted from the molecules. A dehalogenated molecule diffuses on the surface until it finds another dehalogenated molecule, with which it can covalently couple. By designing molecules with different dimensions and with halogens at different sites, one could in principle tailor any type of covalent nanostructures. This is, of course, not the case as there are factors obstructing the assembly process. In particular, self-healing, which is inherent in supramolecular self-assembly, is in general missing, making the assembly into well-ordered two-dimensional covalent networks a formidable task.

Bieri and coworkers identified [2] two processes that are of extra importance for the on-surface synthesis of well-ordered two-dimensional covalent networks, namely the diffusion of dehalogenated molecules and the coupling between two dehalogenated molecules. They defined a recombination probability between two molecules as [2]

$$P_{\text{recomb}} = \frac{v_{\text{couple}}}{v_{\text{couple}} + v_{\text{diffuse}}}, \tag{4}$$

where v_{couple} is the coupling rate and v_{diffuse} is the diffusion rate. It was shown that small recombination probabilities, in other words $v_{\text{diffuse}} \gg v_{\text{couple}}$, are necessary for limiting the number of defects in two-dimensional networks. Later, we have demonstrated that the overall recombination rate may be approximated as [5]

$$v_{\text{recomb}} = \theta \frac{v_{\text{couple}}\, v_{\text{diffuse}}}{v_{\text{couple}} + v_{\text{diffuse}}}, \tag{5}$$

where θ is a parameter depending on the coverage of molecules and the fraction of molecules that has already reacted. This has the implications that the recombination rate is given by

$$v_{\text{recomb}} = \theta v_{\text{couple}} \quad \text{for} \quad v_{\text{diffuse}} \gg v_{\text{couple}}, \tag{6}$$

for coupling-limited processes, and

$$v_{\text{recomb}} = \theta v_{\text{diffuse}} \quad \text{for} \quad v_{\text{diffuse}} \ll v_{\text{couple}}, \tag{7}$$

for diffusion-limited processes.

For a *diffusion-limited process,* the rate of diffusion is much smaller than that of coupling, while for a *coupling-limited process* the rate of diffusion is much larger than that of coupling. For the formation of well-ordered

two-dimensional covalent networks, a *coupling-limited process* is a prerequisite.

Reaction rates are directly related to energy barriers E_{barrier} through the Arrhenius relation

$$v = A \exp[-E_{\text{barrier}}/k_{\text{B}}T], \tag{8}$$

where A is a pre-exponential factor, k_{B} is the Boltzmann's constant, and T the temperature. Knowledge about the barriers of the different processes in the on-surface Ullmann coupling is a necessary step toward the controlled fabrication of covalent materials with this approach. In particular, how the energy barriers depend on the type of molecule and the choice of substrate will aid us choosing the right molecule–surface combination for the assembly of a certain structure. With sufficient amount of information about these reactions, we may be able to derive *rules*, or a chemical intuition, governing the on-surface reactions [3]. Here, we use the formation of biphenyl from halogen-substituted benzene molecules as a model reaction for the on-surface Ullmann coupling. By eventually increasing the complexity of the studied processes, through alteration of the size of, and number of halogens in, the molecule, the trends of the various reaction parameters can be studied, with the intention to arrive at the aforementioned rules/chemical intuition.

3.1 The Formation of Biphenyl from Halogenated Benzenes

We consider the formation of biphenyl from halogenated benzene molecules as a model reaction of on-surface Ullmann coupling. The reaction is divided into three fundamental processes: (i) dehalogenation of the molecular building blocks; (ii) diffusion of dehalogenated molecules; and (iii) coupling of two dehalogenated molecules. The dehalogenation step is described in a separate section, while the diffusion and coupling are described as an overall recombination step because of the reasons discussed above.

3.1.1 Dehalogenation of Bromobenzene and Iodobenzene

The dehalogenation of both bromobenzene and iodobenzene is characterized by an intact physisorbed molecule in the initial state, and a chemisorbed halogen atom and phenyl radical in the final state [5]. The initial and final states are separated by a transition state where the halogenated carbon has initiated a chemical bond with the metal surface and the carbon–halogen bond has begun to break. The initial, transition, and final states are demonstrated for bromobenzene on Ag(111) in Fig. 1,

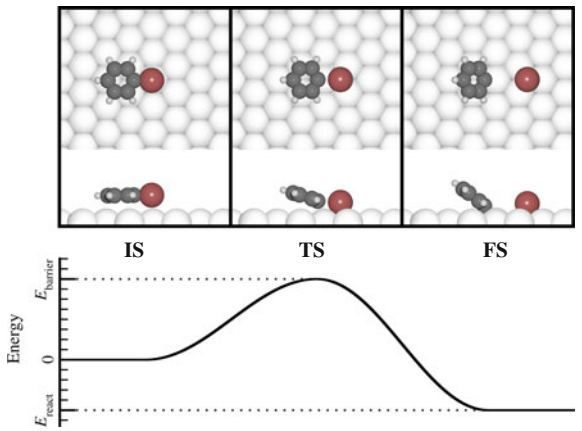

Fig. 1 **a** The dissociation of bromobenzene on Ag(111) showing *top* and *side views* of the initial state (**IS**), transition state (**TS**), and final state (**FS**), exemplifying a typical dehalogenation reaction on a (111)-surface of a noble metal. **b** Representative energy profile of a dehalogenation reaction, indicating the reaction energy (E_{react}) and the energy barrier ($E_{barrier}$) as refined by Eqs. (2) and (3), respectively

and the picture is universal for both bromobenzene and iodobenzene on all the three surfaces Cu(111), Ag(111), and Au(111). Figure 1 also depicts a typical energy profile for a dehalogenation reaction, indicating the reaction energy and energy barrier, as defined by Eqs. (2) and (3), respectively.

Using these definitions of the energy barrier and reaction energy, we can compare these for the different surfaces. Figure 2a shows the energy barrier for bromobenzene and iodobenzene on the three surfaces. Given that both reactions are

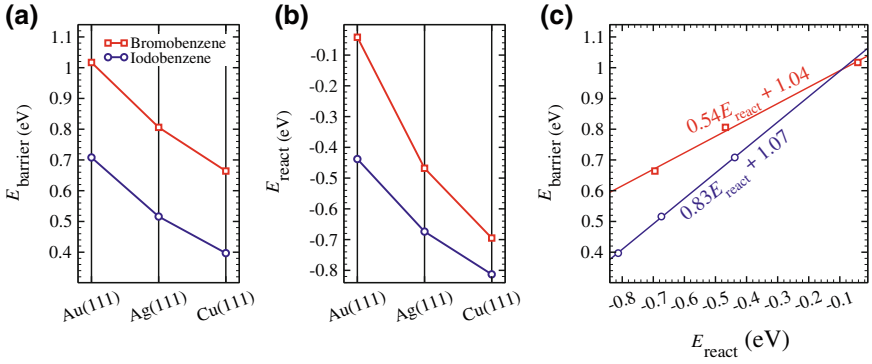

Fig. 2 **a** Energy barriers ($E_{barrier}$) and **b** reaction energies for the dehalogenation of bromobenzene and iodobenzene on the (111)-facets of the coinage metals, as indicated. **c** Relationship between the energy barrier and the reaction energy; the two molecules follow separate Brønsted–Evans–Polanyi relationships. The figure was produced with data from Ref. [5]

highly endothermic in gas phase, with reaction energies of 3.85 and 3.33 eV for bromobenzene and iodobenzene, respectively, it is evident that all the three surfaces have a prominent catalytic effect for abstracting the halogens. For bromobenzene, the barrier ranges from 1.02 eV on Au(111) to 0.66 eV on Cu(111). The exact same trend is found for iodobenzene, with the barriers shifted by roughly 0.3 eV, now ranging from 0.71 eV on Au(111) and 0.40 eV on Cu(111). Interestingly, the reaction energies follow a quite different trend, with a significant larger difference between the two molecules on Au(111) than on Cu(111), as shown in Fig. 2b.

With the small database of reaction characteristics for bromobenzene and iodobenzene, we can investigate the relationship between the reaction energy and the energy barrier. Such a relation would be valuable since reaction energies are much more easily calculated than energy barriers, in the sense of requirements on the computational resources, since we would only need to carry out Step 1 of the recipe in Sect. 2.2. In other words, we would save plenty of time if the energy barrier for a dehalogenation reaction for a given molecule could be estimated directly from the reaction energy. As it turns out, for each of the molecules there exist a Brønsted–Evans–Polanyi relationship; a linear relationship between the energy barrier and the reaction energy

$$E_{\text{barrier}} = aE_{\text{react}} + b, \tag{9}$$

which is illustrated in Fig. 2, where also the values of the parameters a and b are indicated for the two molecules. Importantly, we have to consider the molecules one-by-one to find such a relationship. Thus, there is not a single rule determining the barrier from the reaction energy for dehalogenation reactions, which is not surprising considering that the molecules have different reaction energies in the gas phase. It should be further noted that it is not clear whether the relationship for bromobenzene holds for other brominated molecules (and similar for iodobenzene). One of the objectives of future research will thus be to investigate barriers and reaction energies for other halogenated molecular building blocks, to derive a more general rule for how the barrier height relates to the reaction energy.

To better understand the splitting-off of halogens from molecular precursors, the common step in all on-surface Ullmann coupling schemes, we are encouraged to investigate different types of halogen-substituted molecules. We will build a database of reaction characteristics that can later be used to derive general rules for on-surface dehalogenation reactions.

It is important to point out that dehalogenation on atomically flat surfaces is not necessarily the most realistic model for describing this reaction. In reality, a surface has defects, such as step edges and thermally generated adatoms that diffuse over the terraces of the surface. The latter case may be of particular importance, as it has been shown that on both Cu(110) [11], Cu(111) [19], and Ag(111) [14], following

the dehalogenation but prior to the covalent bond formation, metal-organic networks can be formed with the dehalogenated molecules coordinated to thermally generated adatoms. At this point, we do not know the exact role of these adatoms; whether they participate in the dehalogenation process or form the bond with the dehalogenated molecules at a later stage. This is a question theory should be able to answer during the next few years.

3.1.2 Recombination of Surface-Supported Phenyl Radicals

Following the dehalogenation, the surface-supported radicals will diffuse on the surface until they meet another molecule with which it can covalently couple. Notice the use of the term surface-supported radical. A dehalogenated molecule is formally considered a radical in gas phase. However, due to the strong interaction with the metal surface, its unpaired spin is quenched. This is actually the reason why the dehalogenation barrier is significantly reduced on a metal surface. Thus, in case of on-surface Ullmann coupling a surface-supported radical refers to a dehalogenated molecule interacting chemically with the underlying surface. As previously discussed, both the diffusion and the coupling barriers are of uttermost importance, since they determine whether the overall recombination process is coupling limited or diffusion limited, see the discussion around Eqs. (6) and (7).

The diffusion on Au(111) is slightly different compared to Ag(111) and Cu(111). As shown in Fig. 3, it is a single-barrier process, in which the molecule is standing

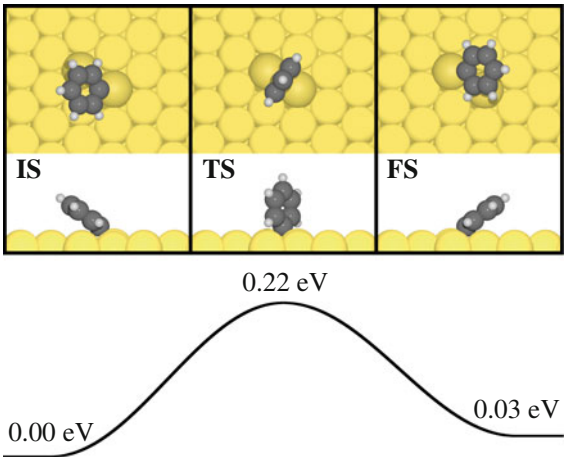

Fig. 3 Diffusion of the phenyl radical on Au(111). The initial, transition, and final states are depicted in (**a**), with the two surface atoms that the phenyl diffuses between rendered darker than other surface atoms. In (**b**) the energy profile is shown for the diffusion with energies indicated with respect to the initial state. The small difference in energy between the initial and the final states is due to difference in adsorption geometry with respect to the subsurface layers. Data from Ref. [5]

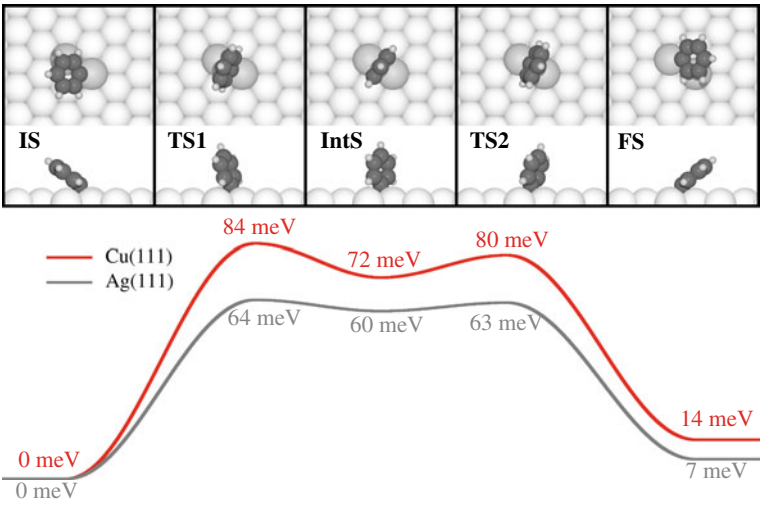

Fig. 4 Diffusion of the phenyl radical on Ag(111) and Cu(111). On both surfaces the initial and final states are separated by an intermediate state and two transition states, depicted for Ag(111) in (**a**). In (**b**) the energy profiles for the two surfaces are shown with energies indicated with respect to the initial state. Data from Ref. [5]

up-right on the surface in the transition state. On the other hand, the diffusion on Ag (111) and Cu(111), illustrated for Ag(111) in Fig. 4a, is a two-barrier process. Similarly to Au(111), the molecule goes through a state where it is standing up-right on the surface, but for Ag(111) and Cu(111) this is a shallow intermediate state in an overall two-step process. It should be noted that the phenyl radical points in opposite direction with respect to the surface in the intermediate and final states for all surfaces such that it is in a way *flipping* across the surface [5], a conclusion that was previously made for the Cu(111) surface [30].

Considering the diffusion barrier, it is significantly larger for Au(111) compared to Ag(111) and Cu(111). For Ag(111) and Cu(111), there also exist an alternative reaction path, in which the molecule has the same orientation in the initial and final states without going through the up-right intermediate state [5]. This may better resemble the behavior for a larger molecule, which will not be able to *flip* between one site and another via an up-right intermediate. In this case, the diffusion barriers on Ag(111) and Cu(111) are increased to 0.29 and 0.44 eV, respectively. This correlates well with the diffusion of the surface-stabilized cyclohexa-*m*-phenylene radical, which has a significantly larger barrier on Cu(111) than Ag(111) [2], while no barrier has been calculated on Au(111).

When two surface-stabilized phenyl radicals are close enough together they may couple to form biphenyl. Figure 5 shows the coupling path of two phenyl radicals given an initial state where the two molecules are chemically bonded to the same surface atom; in other words, they are as close to each other they could possibly be without coupling. The energy profiles in Fig. 5b are given with respect of having

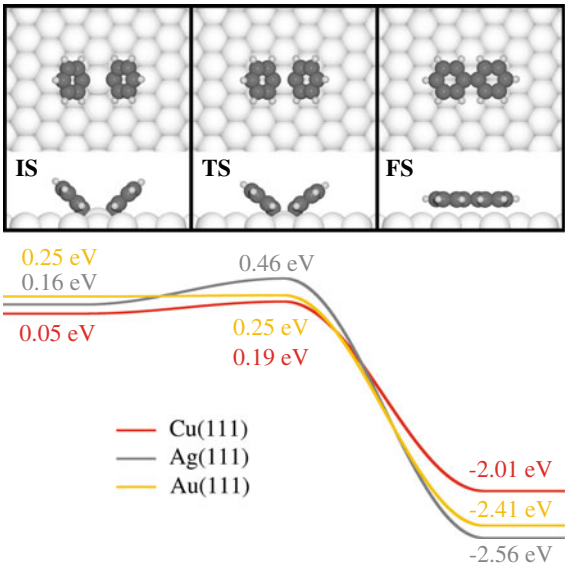

Fig. 5 Coupling of two phenyl radicals into biphenyl, illustrated on Ag(111) in (**a**). The initial state, in which the two phenyls share the same surface atom, and the final state with the molecules covalently coupled are separated by a single transition state. In (**b**) the energy profiles are compared for the reaction on Cu(111), Ag(111) and Au(111). The energies are given with respect to a state where the two molecules are well separated from each other. Notably, on Au(111) there is no barrier separating the initial from the final state. Data from Ref. [5]

the molecules well separated from each other, thus the energy of the initial state gives the net energy cost of bringing the molecules to this position. Notably, on Au (111) there is no barrier separating the initial from the final state. However, the reaction is not spontaneous since one needs to pay a net energy to bring the molecules into the position of the initial state. Also worth noting is that the coupling barrier is largest on Ag(111). The coupling reaction is exothermic with an energy gain larger than 2 eV on all surfaces, resulting from that the carbon–carbon bond is much stronger than a carbon–metal bond. This basically expresses the irreversibility of the coupling reaction.

We previously discussed diffusion-limited versus coupling-limited processes. In case of the biphenyl formation, Ag(111) is the most prominent surface from such an analysis. On this surface, the phenyl diffusion has a barrier of 0.06 eV, while the barrier of the phenyl–phenyl coupling is considerably larger (0.46 eV); in other words, a coupling-limited reaction is expected. In fact, the same conclusions were drawn for the surface-stabilized cyclohexa-*m*-phenylene radical, for which also a coupling-limited process was found on Ag(111) and was also verified from experiments [2].

Similar to the dehalogenation reaction, it will be of great interest to understand how the diffusion and coupling barriers depend on the molecular size and the number of halogen sites. Furthermore, of particular concern will be how adatoms, in

particular on Cu and Ag surfaces, affect these processes. Again, the suggested approach would be to step-wise increase the complexity of the problem and investigate the trends that may emerge. Scrutinizing the trends of diffusion and coupling may be even more crucial than those for dehalogenation considering the importance whether a process is diffusion or coupling limited.

4 Homo-Coupling of Terminal Alkynes

Another type of on-surface reaction that has become quite popular the last few years is the homo-coupling of terminal alkynes. It was first reported as late as 2012 [33] on Ag(111) with the two molecular building blocks 1,3,5-triethynyl-benzene (TEB) and 1,3,5-tris-(4-ethynylphenyl)benzene (Ext-TEB), depicted in Fig. 6a. Since then, it has been demonstrated also with other molecules on different surfaces [9, 10, 13, 16]. The basic principle of the reaction is illustrated in Fig. 6b: Two terminal alkynes couple on a surface together with the release of two hydrogen atoms. An advantage of this coupling scheme compared to the on-surface Ullmann coupling is that the only by-product is in the form of hydrogen instead of halogens.

Regarding the overall reaction process, it has been evidenced that the covalent coupling occurs together with the release of hydrogen [6, 33]. However, as will be discussed in this section, there are fundamental aspects of the reaction mechanism that are not completely clear, and which will require additional attention in the future.

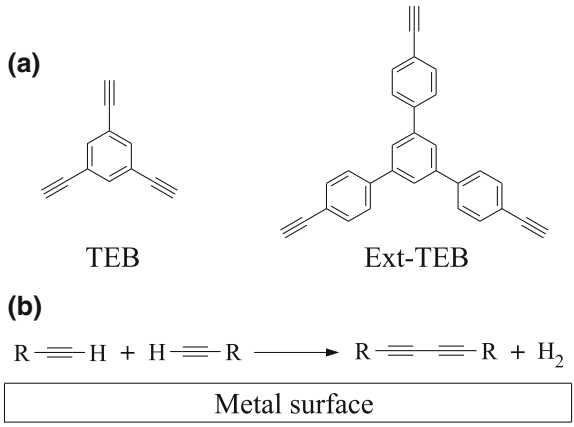

Fig. 6 **a** The molecular building blocks 1,3,5-triethynyl-benzene (TEB) and 1,3,5-tris-(4-ethynylphenyl)benzene (Ext-TEB) that was initially used to demonstrate the homo-coupling of terminal alkynes on Ag(111) [33]. **b** The basic principles of this reaction scheme: terminal alkyne groups of two molecules couple and release hydrogen

4.1 Initial Coupling of Two Molecules

Two independent studies for the reaction mechanisms of the homo-coupling have been carried out [6, 15]. Both studies made the conclusion that instead of removing the hydrogen atoms from the molecular building blocks, the reaction is initiated by the covalent coupling between two molecules. This is illustrated in Fig. 7 for the TEB molecule on Ag(111). Notably, the initial coupling barrier of 0.90 eV is just half the barrier for splitting-off a hydrogen atom directly from a single TEB molecule [6]. Similar values were found for a model component on both the Ag (111) and the Au(111) surfaces [15], and has to be considered as the commonly accepted initial step of the reaction mechanism.

Following the coupling of two TEB molecules on Ag(111), the TEB dimer can exist in two isomeric forms: a trans-isomer (**IntS1**$_{trans}$) in which one carbon is chemically bond to the surface, and a cis-isomer (**IntS1**$_{cis}$) with two carbon atoms chemically bonded to the surface. Considering that the cis-isomer is the considerably more stable of the two, it appears likely that following the initial coupling, the majority of dimers will at some point reside in this form prior to further reactions. The stability of cis-compared to the trans-isomer is due to that the dimer has two carbon atoms chemically bonded in the former while only one in the latter.

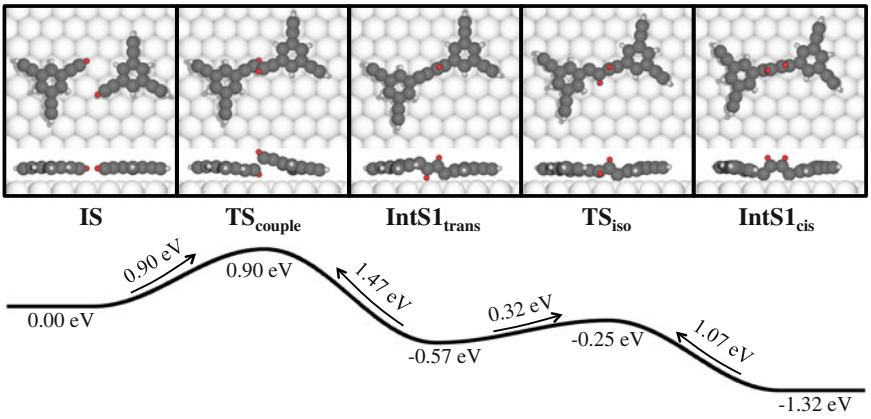

Fig. 7 The homo-coupling of terminal alkynes is initiated by the covalent bond formation between two molecules, with the hydrogen remaining on the molecules, here illustrated for TEB molecules on Ag(111). The coupled intermediate state can exist in a trans- and cis-isomer, where the latter is the more stable one. The two hydrogen atoms taking part in the coupling are shown in red for clarity. Reprinted (adapted) with permission from Ref. [6]. Copyright (2014) American Chemical Society

4.2 Removing Hydrogen from a Covalent Intermediate State

Starting from the cis-isomer of the coupled TEB dimer, one needs to climb two rather large energy barriers, of 1.27 and 1.53 eV, respectively, to split-off the two hydrogen atoms in order to reach the final state of the reaction, shown in Fig. 8. Having in mind that the reaction takes place at temperatures as low as 330 K [33] in particular the second barrier is considerably larger than expected. It is clear that the hydrogen atoms are abstracted following the covalent coupling step; however, it is not completely trivial how. It should be noted that several alternative pathways for removing the hydrogens have been investigated, but without success [6].

One possibility may be that the system has no time to thermally equilibrate following the highly exothermic coupling step. In other words, the energy gained in the coupling is invested into the dehydrogenation steps, reminiscent with the hot adsorbates that can be formed following dissociative adsorption [29]. This would also explain why none of the intermediate states have been observed experimentally. However, to challenge this hypothesis one would need to go beyond basic transition state theory. Importantly, as hydrogen is known to desorb associatively from Ag(111) well below room temperature, the split-off hydrogens will leave the surface and are therefore kinetically hindered to recombine with the molecules.

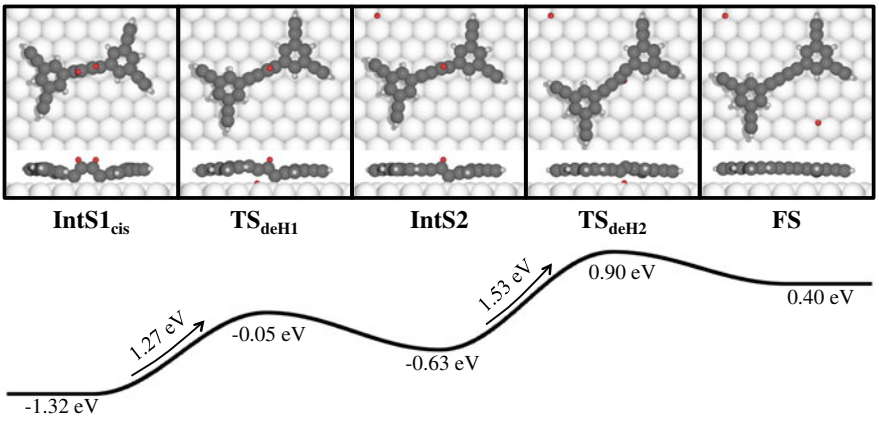

Fig. 8 Following the initial coupling of two TEB molecules, shown in Fig. 7, the dimer undergoes two dehydrogenation steps in order to finalize the overall homo-coupling. The two hydrogen atoms being dehydrogenated are shown in *red* for clarity. Reprinted (adapted) with permission from Ref. [6]. Copyright (2014) American Chemical Society

4.3 *Additional Aspects of the Surface Chemistry of Terminal Alkynes*

It is important to note that the homo-coupling discussed here is not the only possible reaction between terminal alkynes on metals. For example, by using linear molecular building blocks, a variety of products have been obtained on both Au (111) [16] and Ag(111) [10]. In the latter case, the chemoselectivity toward the homo-coupling was retained when using the Ag(887) vicinal surface [10]. The role of the vicinal surface is to *line-up* the molecules along the step edges, effectively quenching other reaction possibilities.

The importance of the underlying surface for controlling the reaction was also demonstrated by Liu and coworkers [26]. Putting the Ext-TEB molecule on Au (111), which on Ag(111) yield the homo-coupling [33], activates a cyclotrimerization reaction, resulting in the formation of a porous graphene structure [26]. Comparisons of the pathways of the cyclotrimerization and homo-coupling are anticipated to provide valuable clues for how to control the chemoselectivity of the multifaceted surface chemistry of terminal alkynes.

5 Outlook

This chapter has given a quite rough overview of how density functional theory can be used to investigate chemical reactions on surface and illustrated a couple of examples where it has been employed for processes relevant for the formation of covalent nanostructures. We have highlighted some of the limitations by considering the formation of biphenyl from halogenated benzenes as model reactions for on-surface Ullmann coupling and it is quite clear that further studies are needed for a more comprehensive theory. For example, we will need to take into account how the dimension of the molecular building blocks, number of halogens per molecule, and positions of halogens within the molecules affect the different reaction steps. This needs to be done systematically, by step-wise increasing the complexity of the studied reaction. When we have reached a critical complexity of the studied systems, patterns will hopefully emerge and we should be able to predict the reaction behavior of far more complex systems, without the requirement to explicitly calculate them.

Whereas the on-surface Ullmann coupling has quite well-defined fundamental reaction steps, where the main challenge remains how to tune the barriers of the various processes, the homo-coupling of terminal alkynes presents a challenge at a more fundamental level. First of all, we do not have the full understanding of how the hydrogen atoms are released in the overall reaction process. Secondly, and maybe more importantly, due to versatile on-surface alkyne chemistry we will need to investigate, and compare, pathways of alternative reactions. This includes not only the cyclotrimerization reaction that has been observed on Au(111) [26], but

also understanding the various reaction products that are formed, particularly for linear molecular building blocks.

This chapter has covered only two of the many possible reaction schemes that can be employed in on-surface synthesis, several of which very limited information about the reaction mechanism exist. During the next decade theoretical surface scientists have a quite daunting, but exciting, task in front of them, to develop accurate and, for experimentalists, useful theories that can be used to bring the field of on-surface synthesis forward, toward a more predictive theory.

Acknowledgements Without the close collaboration with experimental partners, much of the presented work would not have been possible. In particular, Dr. Yi-Qi Zhang, Dr. habil. Florian Klappenberger, and Prof. Johannes Barth at Technische Universität München are acknowledged for their groundbreaking experiments on the homo-coupling of terminal alkynes. Furthermore, I am grateful to Prof. Sven Stafström at Linköping University for encouraging me to follow this exciting line of research.

References

1. Bieri, M., Treier, M., Cai, J., Aït-Mansour, K., Ruffieux, P., Gröning, O., Gröning, P., Kastler, M., Rieger, R., Feng, X., Müllen, K., Fasel, R.: Porous graphenes: two-dimensional polymer synthesis with atomic precision. Chem. Commun., 6919–6921 (2009)
2. Bieri, M., Nguyen, M.-T., Gröning, O., Cai, J., Treier, M., Aït-Mansour, K., Ruffieux, P., Pignedoli, C.A., Passerone, D., Kastler, M., Müllen, K., Fasel, R.: Two-dimensional polymer formation on surfaces: insight into the roles of precursor mobility and reactivity. J. Am. Chem. Soc. **132**, 16669–16676 (2010)
3. Björk, J., Hanke, F.: Towards design rules for covalent nanostructures on metal surfaces. Chem. Eur. J. **20**, 928–934 (2014)
4. Björk, J., Stafström, S.: Adsorption of large hydrocarbons on coinage metals: a van der Waals density functional study. ChemPhysChem **15**, 2851–2858 (2014)
5. Björk, J., Hanke, F., Stafström, S.: Mechanisms of halogen-based covalent self-assembly on metal surfaces. J. Am. Chem. Soc. **135**, 5768–5775 (2013)
6. Björk, J., Zhang, Y.-Q., Klappenberger, F., Barth, J.V., Stafström, S.: Unraveling the mechanism of the covalent coupling between terminal alkynes on a noble metal. J. Phys. Chem. C **118**, 3181–3187 (2014)
7. Bürker, C., Ferri, N., Tkatchenko, A., Gerlach, A., Niederhausen, J., Hosokai, T., Duhm, S., Zegenhagen, J., Koch, N., Schreiber, F.: Exploring the bonding of large hydrocarbons on noble metals: diindoperylene on Cu(111), Ag (111), and Au (111). Phys. Rev. B **87**, 165443–165447 (2013)
8. Cai, J., Ruffieux, P., Jaafar, R., Bieri, M., Braun, T., Blankenburg, S., Muoth, M., Seitsonen, A.P., Saleh, M., Feng, X., Müllen, K., Fasel, R.: Atomically precise bottom-up fabrication of graphene nanoribbons. Nature **466**, 470–473 (2010)
9. Cirera, B., Zhang, Y.-Q., Klyatskaya, S., Ruben, M., Klappenberger, F., Barth, J.V.: 2D self-assembly and catalytic homo-coupling of the terminal alkyne 1,4-Bis (3,5-diethynyl-phenyl)butadiyne-1,3 on Ag(111). ChemCatChem **5**, 3281–3288 (2013)
10. Cirera, B., Zhang, Y.-Q., Björk, J., Klyatskaya, S., Chen, Z., Ruben, M., Barth, J.V., Klappenberger, F.: Synthesis of extended graphdiyne wires by vicinal surface templating. Nano Lett. **14**, 1891–1897 (2014)

11. Di Giovannantonio, M., El Garah, M., Lipton-Duffin, J., Meunier, V., Cardenas, L., Fagot Revurat, Y., Cossaro, A., Verdini, A., Perepichka, D.F., Rosei, F., Contini, G.: Insight into organometallic intermediate and its evolution to covalent bonding in surface-confined Ullmann polymerization. ACS Nano **7**, 8190–8198 (2013)
12. Dion, M., Rydberg, H., Schröder, E., Langreth, D.C., Lundqvist, B.I.: Van der Waals density functional for general geometries. Phys. Rev. Lett. **92**, 246401–246404 (2004)
13. Eichhorn, J., Heckl, W.M., Lackinger, M.: On-surface polymerization of 1,4-diethynylbenzene on Cu(111). Chem. Commun. **49**, 2900–2902 (2013)
14. Eichhorn, J., Strunskus, T., Rastgoo-Lahrood, A., Samanta, D., Schmittele, Lackinger, M.: On-surface Ullmann polymerization via intermediate organometallic networks on Ag(111). Chem. Commun. **50**, 7680–7682 (2014)
15. Gao, H.-Y., Franke, J., Wagner, H., Zhong, D., Held, P.-A., Studer, A., Fuchs, H.: Effect of metal surfaces in on-surface glaser coupling. J. Phys. Chem. C **117**, 18595–18602 (2013)
16. Gao, H.-Y., Wagner, H., Zhong, D., Franke, J.-H., Studer, A., Fuchs, H.: Glaser coupling at metal surfaces. Angew. Chem. Int. Ed. **52**, 4024–4028 (2013)
17. Grill, L., Dyer, M., Lafferentz, L., Persson, M., Peters, M.V., Hecht, S.: Nano-architectures by covalent assembly of molecular building blocks. Nature Nanotechnol. **2**, 687–891 (2007)
18. Grimme, S.: Semiempirical GGA-type density functional constructed with a long-range dispersion correction. J. Comp. Chem. **27**, 1787–1799 (2006)
19. Gutzler, R., Walch, H., Eder, G., Kloft, S., Hecklab, W.M., Lackinger, M.: Surface mediated synthesis of 2D covalent organic frameworks: 1,3,5-Tris(4-Bromophenyl)benzene on graphite (001), Cu(111), and Ag(110). Chem. Commun. **45**, 4456–4458 (2009)
20. Henkelman, G., Jónsson, H.: A dimer method for finding saddle points on high dimensional potential surfaces using only first derivatives. J. Chem. Phys. **111**, 7010–7022 (1999)
21. Henkelman, G., Jónsson, H.: Improved tangent estimate in the nudged elastic band method for finding minimum energy paths and saddle points. J. Chem. Phys. **113**, 9978–9985 (2000)
22. Henkelman, G., Uberuaga, B.P., Jónsson, H.: A climbing image nudged elastic band method for finding saddle points and minimum energy paths. J. Chem. Phys. **113**, 9901–9904 (2000)
23. Kästner, J., Sherwood, P.: Superlinearly converging dimer method for transition state search. J. Chem. Phys. **128**, 014106–014111 (2008)
24. Kohn, W., Sham, L.J.: Self-consistent equations including exchange and correlation effects. Phys. Rev. **140**, A1133–A1138 (1965)
25. Lafferentz, L., Eberhardt, V., Dri, C., Africh, C., Comelli, G., Esch, F., Hecht, S., Grill, L.: Controlling on-surface polymerization by hierarchical and substrate-directed growth. Nature Chem. **4**, 215–220 (2012)
26. Liu, J., Ruffieux, P., Feng, X., Müllen, K., Fasel, R.: Cyclotrimerization of arylalkynes on Au (111). Chem. Commun. **50**, 11200–11203 (2014)
27. Logadottir, A., Rod, T.H., Nørskov, J.K., Hammer, B., Dahl, S., Jacobsen, C.J.H.: The BrønstedEvansPolanyi relation and the volcano plot for ammonia synthesis over transition metal catalysts. J. Catal. **197**, 229–231 (2001)
28. Matena, M., Björk, J., Wahl, M., Lee, T.-L., Zegenhagen, J., Gade, L.H., Jung, T.A., Persson, M., Sthr, M.: On-surface synthesis of a two-dimensional porous coordination network: unraveling adsorbate interactions. Phys. Rev. B **90**, 125408–125415 (2014)
29. Meyer, J., Reuter, K.: Modeling heat dissipation at the nanoscale: an embedding approach for chemical reaction dynamics on metal surfaces. Angew. Chem. Int. Ed. **53**, 4721–4724 (2014)
30. Nguyen, M.-T., Pignedoli, C.A., Passarone, D.: An Ab initio insight into the Cu(111)-mediated Ullmann reaction. Phys. Chem. Chem. Phys. **13**, 154–160 (2011)
31. Ruiz, V., Liu, W., Zojer, E., Scheffler, M., Tkatchenko, A.: Density-functional theory with screened van der Waals interactions for the modeling of hybrid inorganic-organic systems. Phys. Rev. Lett. **108**, 146103–146107 (2012)
32. Thonhauser, T., Cooper, V.R., Li, S., Puzder, A., Hyldgaard, P., Langreth, D.C.: Van der Waals density functional: self-consistent potential and the nature of the van der Waals bond. Phys. Rev. B **76**, 125112–125122 (2007)

33. Zhang, Y.-Q., Kepčija, N., Kleinschrodt, M., Diller, K., Fischer, S., Papageorgiou, A.C., Allegretti, F., Björk, J., Klyatskaya, S., Klappenberger, F., Ruben, M., Barth, J.V.: Homo-coupling of terminal alkynes on a noble metal surface. Nat. Commun. **3**, 1286 (2012)
34. Xi, M., Bent, B.E.: Iodobenzene on Cu(111): formation and coupling of adsorbed phenyl groups. Surf. Sci. **278**, 19–32 (1992)